DESIGN AND FABRICATION REQUIREMENTS FOR LOW NOISE SUPERSONIC/HYPERSONIC WIND TUNNELS

I. E. Beckwith
NASA Langley Research Center
Hampton, Virginia

F.-J. Chen and M. R. Malik
High Technology Corporation
Hampton, Virginia

PROPOSED SUPERSONIC LOW-DISTURBANCE TUNNEL

A schematic diagram of the new proposed Supersonic Low-Disturbance Tunnel at NASA Langley is shown in figure 1. Existing high pressure air and vacuum systems will be used. The specifications and design of two high quality air filters for the new facility are based on experiences and data in the pilot tunnel (ref. 1). Aerodynamic analysis and engineering details of the 8-ft diameter settling chamber and other tunnel components are given in reference 2. The tunnel is designed to accommodate nozzles of various lengths with Mach numbers ranging from 2 to 6. The first nozzle to be operated in the tunnel will be the Mach 3.5 rapid expansion, two-dimensional nozzle illustrated in the lower part of figure 1. The two-stroke model injector is required to place the model into the quiet test core in the upstream part of the uniform flow test rhombus. A 1/3-scale version of this nozzle has been developed and tested extensively in the Pilot Low-Disturbance Tunnel at NASA Langley (refs. 1-4). The techniques for obtaining laminar boundary layers on the nozzle walls, which is the key requirement for quiet test section flow, will be presented in the next several figures.

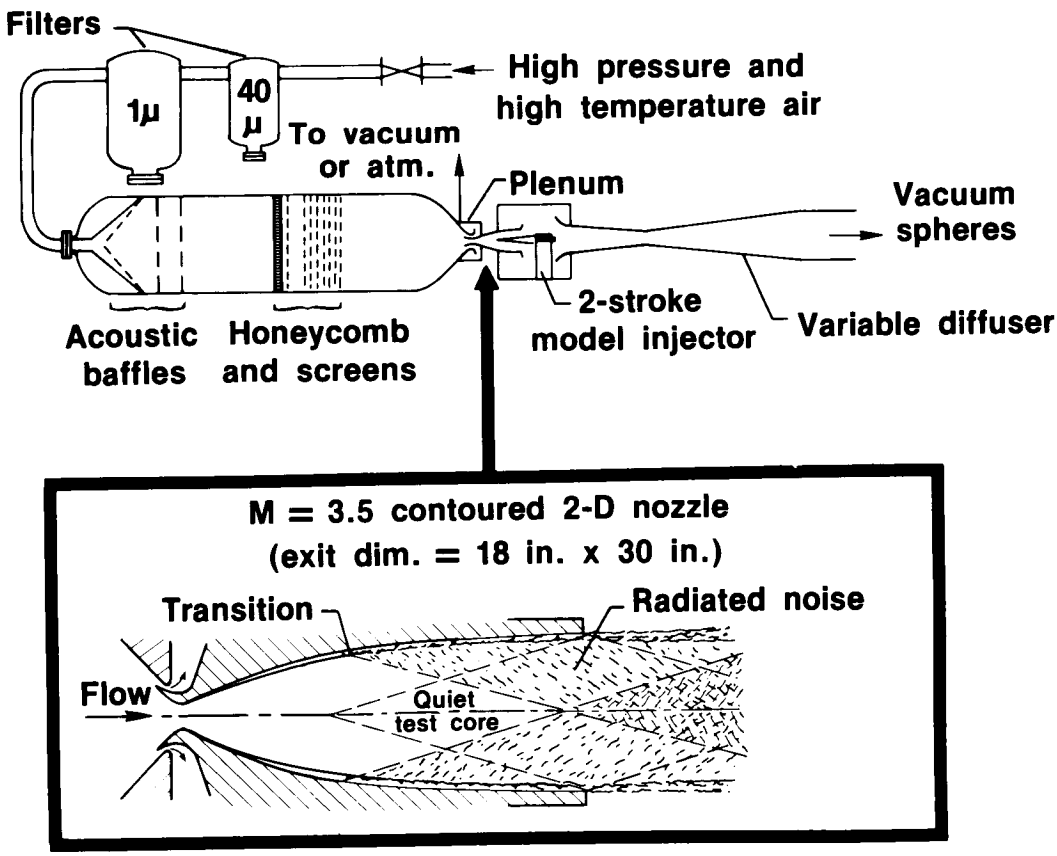

Figure 1

QUIET TEST CORE IN M_∞ = 3.5 RAPID EXPANSION NOZZLE

The dominant source of test-section disturbances in conventional supersonic/hypersonic tunnels is the acoustic radiation from eddies in the turbulent boundary layers on the nozzle walls. In supersonic flow, this noise is in the form of finite-strength wavelets which are propagated along Mach lines. Hence, as illustrated in figure 2, the location of transition onset in the wall boundary layers is sensed with a hot-wire probe at any point along a Mach line extended downstream from that location which is then the "acoustic origin" for the onset of radiated noise in the nozzle flow field. As the unit Reynolds number is increased, transition moves upstream along the contoured walls in this nozzle. The quiet test core region then becomes smaller and tends to approach some minimum size of streamwise length ΔX and height ΔY. When the nozzle walls are very clean and highly polished, the minimum value of ΔX is about 4.5-inches (refs. 1 and 2). At high Reynolds numbers, the sidewall boundary layers are generally turbulent. For these conditions, radiation from the side walls is minimized by the large width of the nozzle (see lower part of fig. 2) and the small local Mach numbers ($M_e < 2.5$) at the acoustic origin locations. The large width of the quiet test core, ΔZ, allows the testing of swept wings and models at large angle of attack.

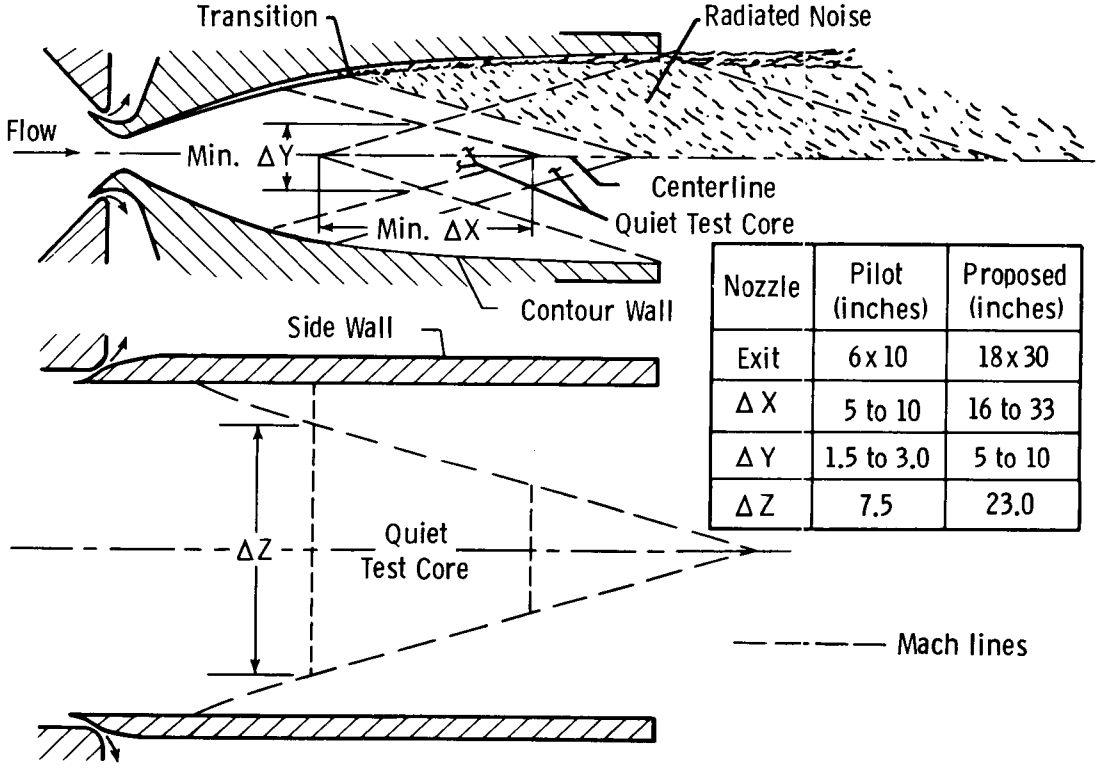

Nozzle	Pilot (inches)	Proposed (inches)
Exit	6 x 10	18 x 30
Δ X	5 to 10	16 to 33
Δ Y	1.5 to 3.0	5 to 10
Δ Z	7.5	23.0

Figure 2

TRANSITION REYNOLDS NUMBERS ON SHARP CONES

Local Reynolds numbers at transition onset, Re_T, determined from recovery temperatures measured on a sharp tip 5° half-angle cone in the pilot tunnel are plotted against local unit Reynolds number, Re, in figure 3 (see refs. 3 and 4). For values of Re/in < 8 x 10^5, these data are in the range of atmospheric flight data which are much higher than conventional wind-tunnel data due to the high-stream noise levels in these latter tunnels (sources of these flight and conventional wind-tunnel data are given in ref. 3). The cone used in the quiet tunnel tests was 15-inches long, and for these lower values of Re/in, transition usually occurred on the cone well downstream of the acoustic origin boundary of the quiet test core. Analysis and correlation of these results (refs. 3 and 5) indicate that the cone boundary layer is much more sensitive to wind-tunnel noise in the vicinity of the neutral stability point than further downstream. For Re/in > 8 x 10^6, the transition Reynolds numbers decrease more or less rapidly towards the levels for previous conventional wind-tunnel data depending on the nozzle wall finish. The effect of surface finish on wall transition and quiet test core sizes in the pilot nozzle and the corresponding quantitative requirements on the wall finish will be considered next.

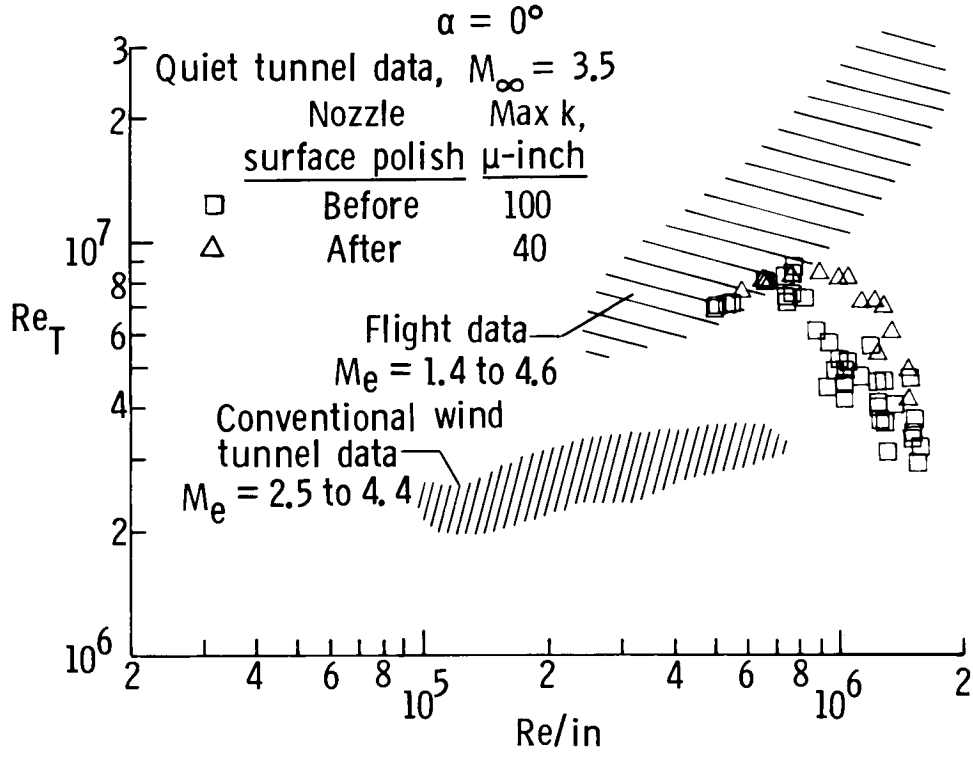

Figure 3

EFFECT OF TRANSITION ON QUIET TEST CORE LENGTH

Figure 4 shows how the axial distance from the throat to transition on the nozzle wall, X_T, is related to the length of the quiet test core, ΔX. Values of these parameters and corresponding free-stream Reynolds numbers based on ΔX are given in the table for large values of $R_\infty/in > 9 \times 10^5$ and for different surface finish conditions. The original blocks were made of 17-4 PH stainless steel with a nominal surface finish of 4 to 6 rms μ-inches. After more polish work was completed the finish was improved to about 1 rms μ-inch and the values of ΔX then approached the "minimum" values observed for this very good surface finish with the corresponding much larger values of $R_{\infty,\Delta X}$. As part of an attempt to improve this finish a new set of blocks was machined from 15-5 PH vacuum remelt stainless steel. The before-polish data on these blocks indicates that ΔX was very small or zero. After preliminary polish work, the value of ΔX for $R_\infty/in \approx 10 \times 10^5$ was increased by a factor of about 7 times. However, at $R_\infty/in = 12.5 \times 10^5$ there was still no usable quiet test core. To understand the reasons for these poor results, we will consider next the effects of known roughness magnitudes and characteristics on nozzle-wall transition.

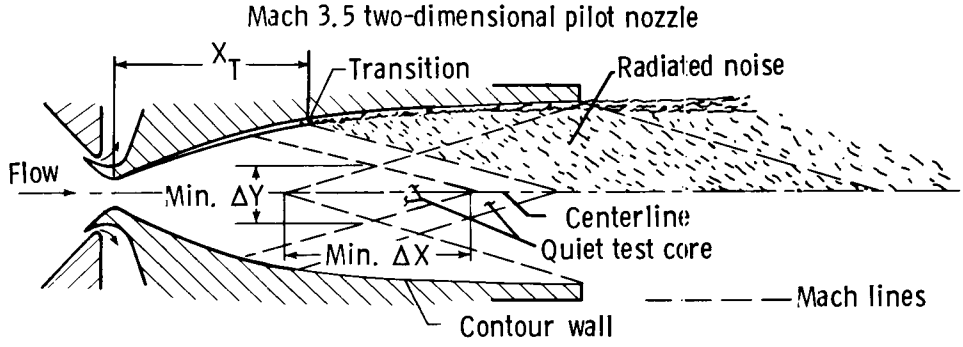

	$R_\infty/in. \times 10^{-5}$	X_T, inches	Quiet ΔX, inches	$R_{\infty,\Delta X} \times 10^{-6}$	
Original blocks	10.2	1.7	2.5	2.6	Before Polish
	15.0	.9	.5	.8	
	10.4	2.7	4.6	4.8	After Polish
	15.5	2.6	4.5	7.0	
New blocks	10.0	1.0	0.7	0.7	Before
	15.1	0.6	0	0	
	9.3	2.9	4.9	4.6	After
	12.5	0.4	0	0	

Figure 4

EFFECT OF SURFACE DAMAGE ON TRANSITION ASYMMETRY

The surface finish of the new Mach 3.5 two-dimensional nozzle blocks has been monitored throughout the polish work with scanning micro-video-recording equipment developed by Dr. L. M. Weinstein at NASA Langley. The effects of any observed surface defects on nozzle-wall boundary-layer transition can then be determined from hot-wire surveys of free-stream disturbances. Results of such surveys obtained after the preliminary polish work (fig. 4) are shown in figure 5. These surveys were made in the vertical centerplane of the nozzle along the centerline (Y = 0) and 1/2-inch above the centerline (Y = 1/2-inch) as illustrated in the upper part of the figure. In the lower part of the figure, values of the rms pressure normalized by the mean static pressure, $\tilde{P}/\bar{P}$, (the "noise level") from the hot-wire data are plotted against the axial distance from the throat for three unit Reynolds numbers. The criterion used to locate transition is where the noise levels rise above low "laminar" values to $\tilde{P}/\bar{P}$ = 0.1 percent. In the upper part of the figure, the asymmetrical locations of transition on the top (No. 1) and bottom (No. 2) blocks are shown for the surveys at $R_\infty/\text{in} = 3.7 \times 10^5$. The arrow indicates where transition would have been detected at Y = 1/2-inch for symmetrical locations on the two blocks. The three arrows in the lower part of the figure indicate where transition would be for the surveys at Y = 1/2-inch if X_T was the same on both blocks for the three unit Reynolds numbers. At the highest unit Reynolds number of 9.6×10^5/in, transition asymmetry is more pronounced and $(X_T)_{Y=0}$ = 6.2-inches which corresponds to X_T = 1.1-inch on the wall of block No. 2. This location of transition is well upstream of its location at the slightly smaller value of $R_\infty/\text{in} = 9.3 \times 10^5$ in figure 4 where X_T = 2.9-inches. This rapid forward movement of transition with increasing unit Reynolds number and the consistently larger values of X_T on block No. 1 than block No. 2, as well as the complete loss of laminar flow at $R_\infty/\text{in} = 12.5 \times 10^5$ (fig. 4) are caused by different surface defects on the two blocks as shown in the next two figures.

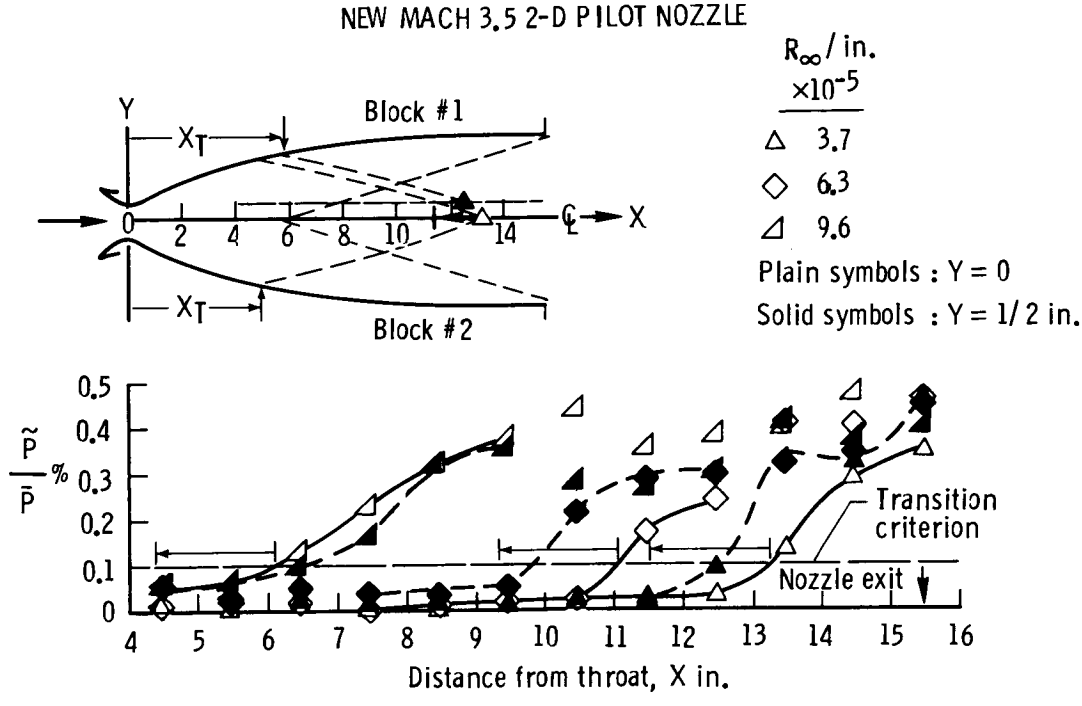

Figure 5

POLISH RESULTS ON NEW MACH 3.5 TWO-DIMENSIONAL NOZZLE
BLOCK NO. 1

Figure 6 shows four microphotographs which illustrate the gradually improved surface finish as the diamond polish grit is reduced in size from 15 microns down to 1/4-micron. A typical pattern of pits located at X = .7-inch from the throat and at Z = 5.1-inches from the sidewall on block No. 1 is shown. Most of these pits are probably caused by micro-inclusions (air bubbles) in the metal. The larger pits in the photographs are .002 to .004-inch long with depths up to about 120 μ- inches measured with a micro-deflection transducer attached to the scanning video microscope. A large amount of data obtained with a commercial profilometer on these blocks indicates that some of the smaller pits are only 20 to 30 microinches deep and that the number and size of the pits decreases as the throat region is approached.

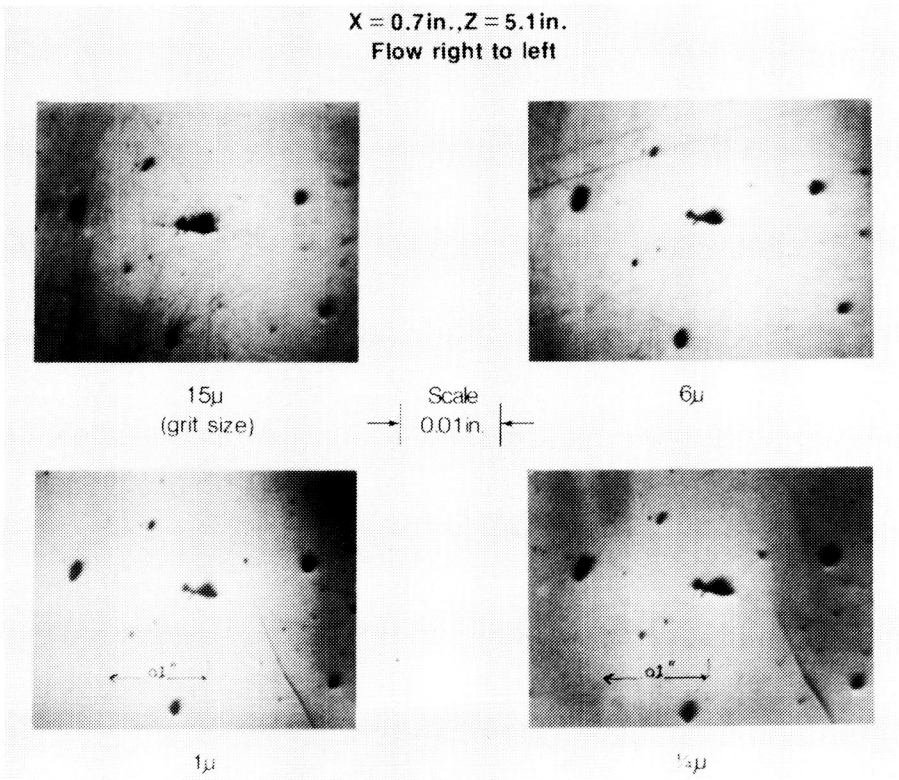

Figure 6

DAMAGE TO SURFACE FINISH FROM POLISH CONTAMINANTS

Figure 7 shows two microphotographs and corresponding profilometer traces of typical contaminant scratches which were visible to the naked eye and were observed only on block No. 2. These scratches, as well as many pits (fig. 6), were present during the test runs used for figures 4 and 5. The scratches shown in figure 7 are only 30 to 35 micro-inches deep at the location of the profilometer stylus tracks. However, they are close to the throat and are aligned across the flow direction. (The laminar boundary-layer thicknesses for $R_\infty = 10 \times 10^5$/inch at these two locations of X = .1 and .3-inch were only .002 and .003-inch, respectively). We conclude from these results and the transition asymmetry shown on figure 5 where X_T was consistently smaller on block No. 2 than block No. 1, that scratches of this type and depth are more dangerous than pits (fig. 6) to the required maintenance of laminar boundary layers on these nozzle walls.

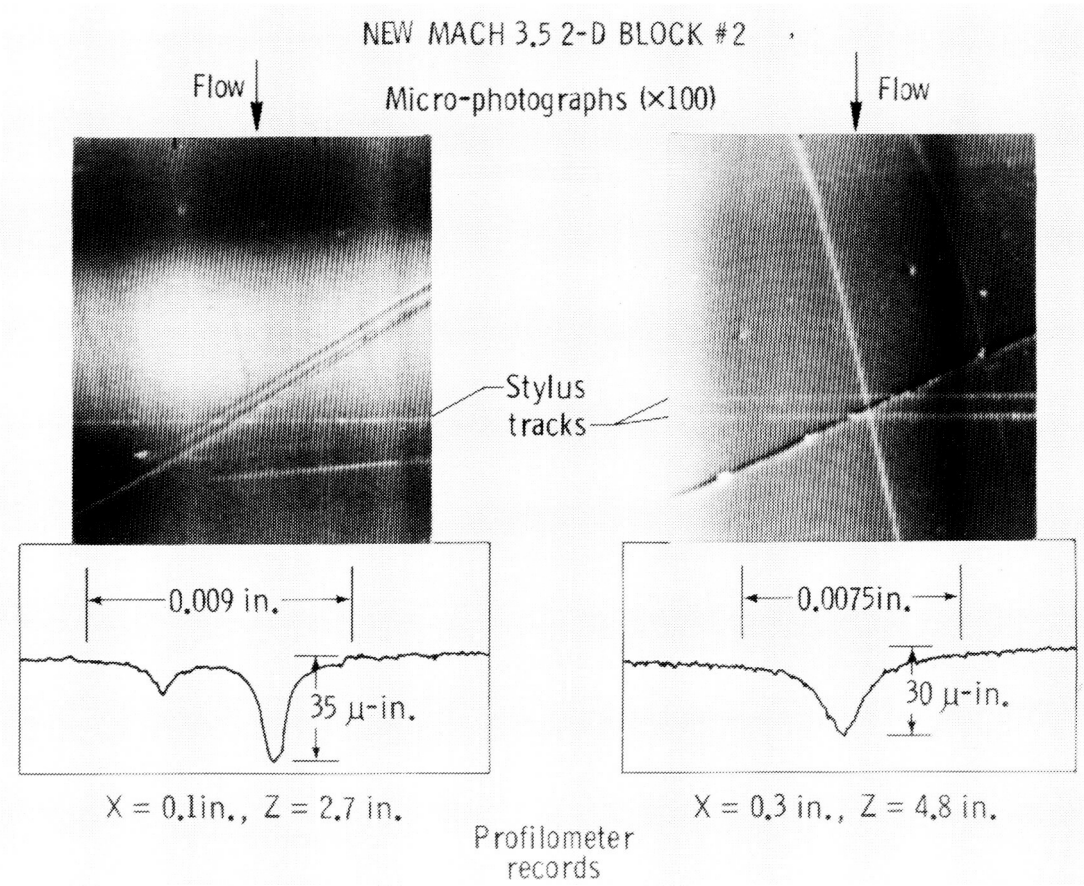

Figure 7

ALLOWABLE SURFACE ROUGHNESS

A review of profilometer roughness measurements on both the original and new Mach 3.5 two-dimensional contoured nozzle blocks is presented in figure 8. The maximum peak-to-valley roughness defects, k, obtained from profilometer measurements on these blocks before and after polish work are plotted against the axial distance from the throat. Typical data at different distances from the sidewall are shown. These data may be compared with the calculated variations of k obtained from numerical solutions for the local laminar boundary-layer profiles using the computer code of reference 6 for the two values of R_∞ shown and for the two values of roughness "height" Reynolds numbers of R_k = 42 and 12. This type of roughness Reynolds number, defined as the local Reynolds number evaluated at the distance from the surface of y = k, has been used historically to characterize the effects of both isolated and distributed roughness particles on transition. Early examples are given in reference 7 where critical values of R_k for transition on flat plates and cones varied from about 260 to 625 for the Mach number range from 1.6 to 3.7. The critical values of R_k on these blocks are apparently much smaller, presumably due to the different type of roughness and the different flow conditions such as pressure gradients and instability mechanisms. Nevertheless, it may be concluded from detailed flow and roughness data in references 1-4 and the results in figures 4-7 herein, that $R_k \simeq 10$ is required to maintain laminar boundary layers on the contoured walls in this type of nozzle. For this application, k is defined as the maximum peak-to-valley profilometer measurement of local surface defects. However, all scratches of the type shown in figure 7 must be removed during the final polishing work.

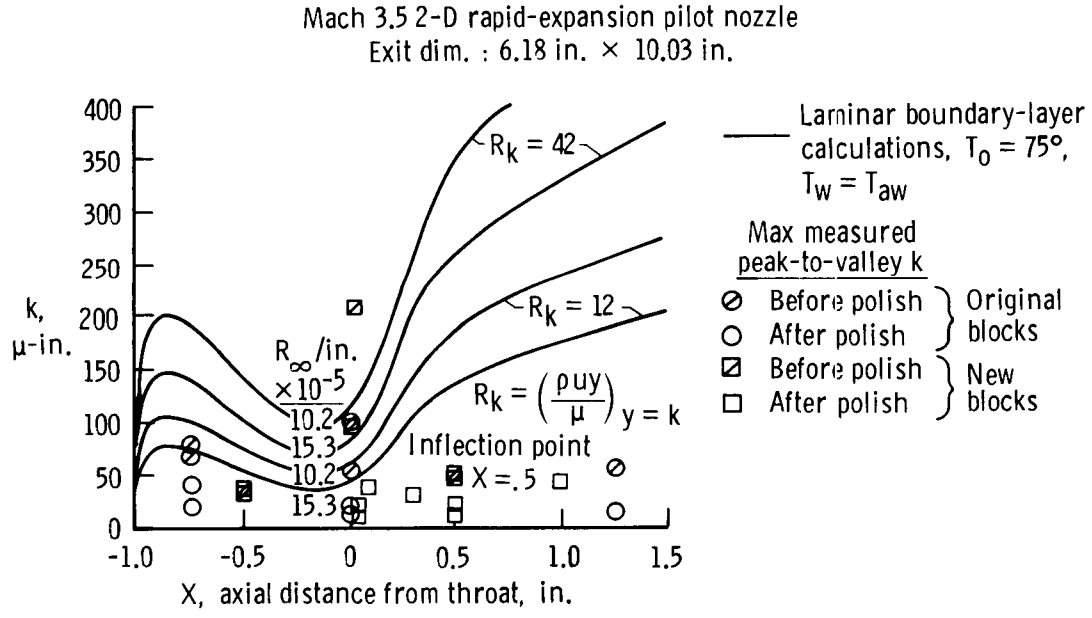

Figure 8

GÖRTLER VORTICES IN M=3.5 TWO-DIMENSIONAL NOZZLE

In order to apply transition results from the present nozzles to the design of different nozzles at other flow conditions or to more general supersonic configurations, it is essential to understand the transition mechanisms involved and to develop theoretical models that can be used for predictive purposes. An early start to understanding the mechanisms was reported in reference 8, but satisfactory models depended on the successful application of linear stability theory by Dr. Malik to the correct local flow conditions (refs. 4, 9 and 10). The principal results of this work were to show that transition in these nozzles for Mach numbers from 3 to 5 was generally caused by the Gőrtler instability mechanism in the concave curvature regions of the nozzles rather than Tollmien-Schlichting waves, provided that the nozzle walls were maintained clean and polished, and boundary-layer removal slots at the nozzle entrance were used. A brief review of some of that work will now be presented with applications to the design of advanced nozzles that promise much longer quiet test regions than achieved to date.

Figure 9 shows flow vectors calculated by the stability theory for Görtler vortices (the mean flow direction is into the page) in the Mach 3.5 two-dimensional pilot nozzle at $R_\infty = 5.1 \times 10^5$/in, where the experimental location of transition on the wall was at $X_{w,T}$ = 3.6-inches from the throat. The laminar boundary-layer thickness at this point was 0.019-inch and maximum amplification was calculated when the ratio of Görtler wavelength to boundary-layer thickness, λ/δ, was taken as 0.82 as shown on the right side of the figure. These conditions gave N = 9.6 as the integral of the local amplification rates from the wall inflection point to transition.

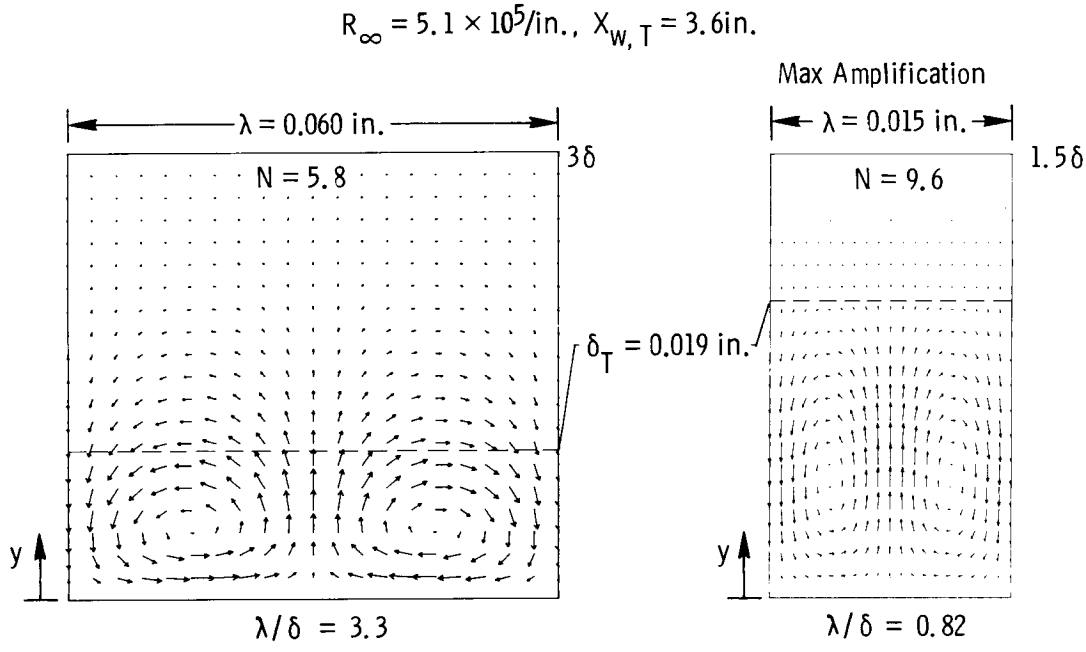

Figure 9

EFFECT OF GÖRTLER VORTEX WAVELENGTH ON AMPLIFICATION TO TRANSITION

Figure 10 shows that the N-factors for maximum amplification to transition of the Görtler vortices in this nozzle varied from about 9 to 11 over the entire range of test Reynolds numbers and measured transition locations, $X_{w,T}$. These transition locations were observed only when the nozzle walls were clean and polished and with the bleed valve open (ref. 4). The calculated maximum amplification always occurred within the narrow wavelength range of $.75 < \lambda/\delta < .95$. Similar results were obtained in two rapid-expansion axisymmetric nozzles for test section Mach numbers of 3 and 5 (ref. 10).

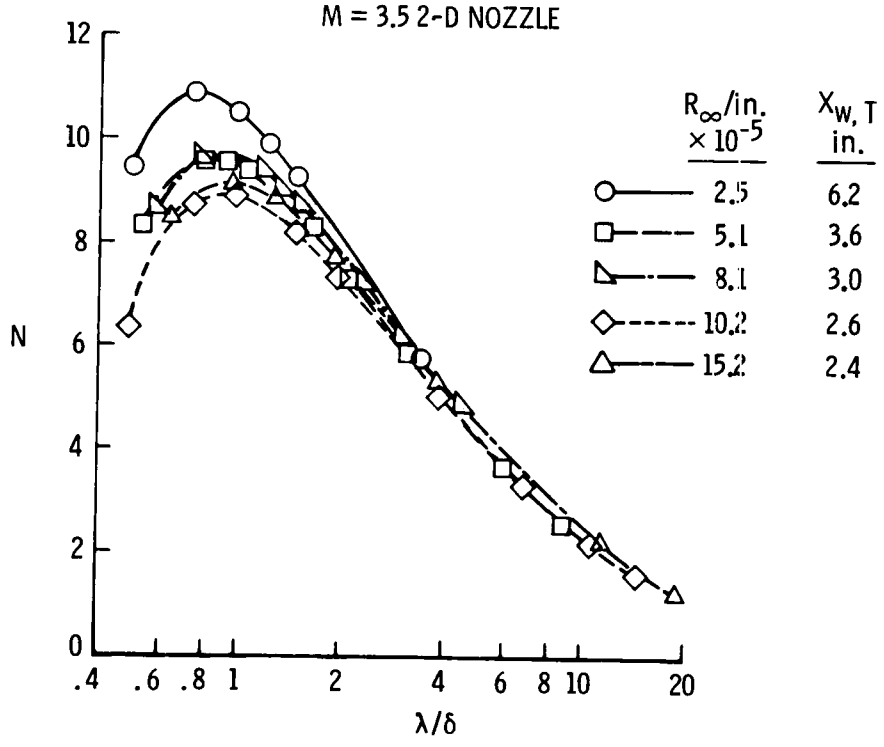

Figure 10

MACH 3.5 AXISYMMETRIC-LONG NOZZLE

After it was established that Görtler vortices were the dominant cause of transition in these slotted nozzles, techniques for modifying the onset and amplification of the vortices were developed (ref. 4, 9, and 10). The most practical technique was to insert a section of radial flow in the expansion region of the nozzle. This technique is used to minimize the concave wall curvature by moving the inflection point far downstream which delays the onset of the Görtler instability and reduces the vortex growth rates because of smaller streamwise increases in boundary-layer thicknesses.

Figure 11 illustrates the application of this technique to the aerodynamic design of a new Mach 3.5 axisymmetric nozzle which is now being fabricated. The value of the N-factor used to predict the location of transition ($X_{w,T}$) was taken as N = 9.2. At the largest value of R_∞/in = 15.5 x 10^5, the value of N for amplification of Tollmien-Schlichting (TS) waves was only 2.3. Therefore, if the surface finish determined by the criteria of $R_k \simeq 10$ can be obtained, and if the extremely small tolerances on wall radius and waviness based on our test results of a Mach 3 rapid-expansion axisymmetric nozzle (ref. 10) can be achieved, this new nozzle should provide the large values of $R_{\infty,\Delta X}$ shown.

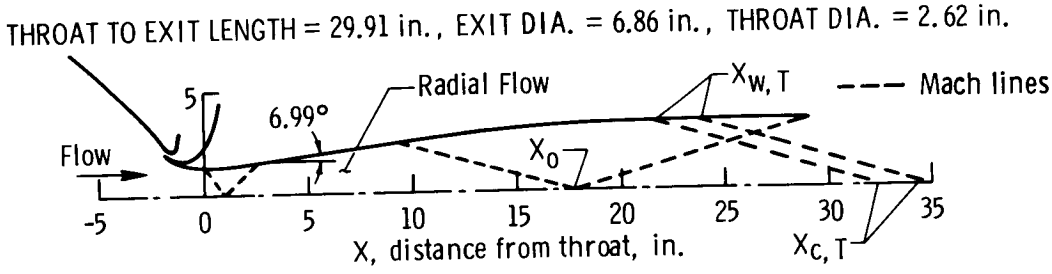

Transition predicted for Görtler N = 9.2, T_0 = 530°R

P_0 psia	R_∞/in. $\times 10^{-6}$	$X_{w,T}$ inches	$X_{c,T}$ inches	$\Delta X = X_{c,T} - X_0$, in.	$R_{\infty,\Delta X}$ $\times 10^{-6}$	TS N
100	1.03	23.57	34.89	17.09	17.6	
150	1.55	21.21	32.40	14.60	22.6	2.3

Figure 11

COMPARISON OF TRANSITION REYNOLDS NUMBERS WITH $R_{\Delta X}$

Experimental values of $R_{\Delta X}$ for three nozzles are compared with flight data for transition Reynolds numbers, R_T, on cones in figure 12. The Mach 3 axisymmetric rapid-expansion nozzle (ref. 10) was fabricated by electroforming nickel onto a stainless steel mandrel. The final surface finish of the mandrel was examined with an interference microscope. The space between each fringe was 10.75 micro-inches, or half the wavelength of the green mercury light used. The maximum peak-to-valley defects as determined from the fringe deviations on micro-interferograms at 6 random locations on the mandrel was approximately 15 μ-inches. The electroformed nickel surface of the nozzle duplicated that of the mandrel and resulted in the highest quality finish on any of the 6 nozzles tested to date. The measured values of $R_{\Delta X}$ were also higher than for the other nozzles. At the highest test unit Reynolds number of $R_\infty = 1.6 \times 10^6$/in, $R_{\Delta X} = 10.1 \times 10^6$ for the Mach 3 nozzle. The calculated value of the N-factor at the corresponding measured location of transition was N = 5.9 (ref. 10). The effects of different surface finishes, as shown in figure 8, on $R_{\Delta X}$ for both the original and new Mach 3.5 two-dimensional, rapid expansion (R.E.) blocks are also shown in figure 12. Note that the new blocks with maximum k = 40 μ-inches, resulted in the highest levels of $R_{\Delta X}$ for R_∞/in < 6×10^5/inch. However, for R_∞/in > 9.3×10^5 the extent of laminar flow decreased rapidly due to the influence of damage scratches such as those shown in figure 7. The predicted values of $R_{\Delta X}$ for the new axisymmetric-long Mach 3.5 nozzle are in the range of flight data for R_T. This indicates that most of the laminar boundary layer preceding transition on slender test models would be exposed to the extremely low "laminar" noise levels below .05 percent.

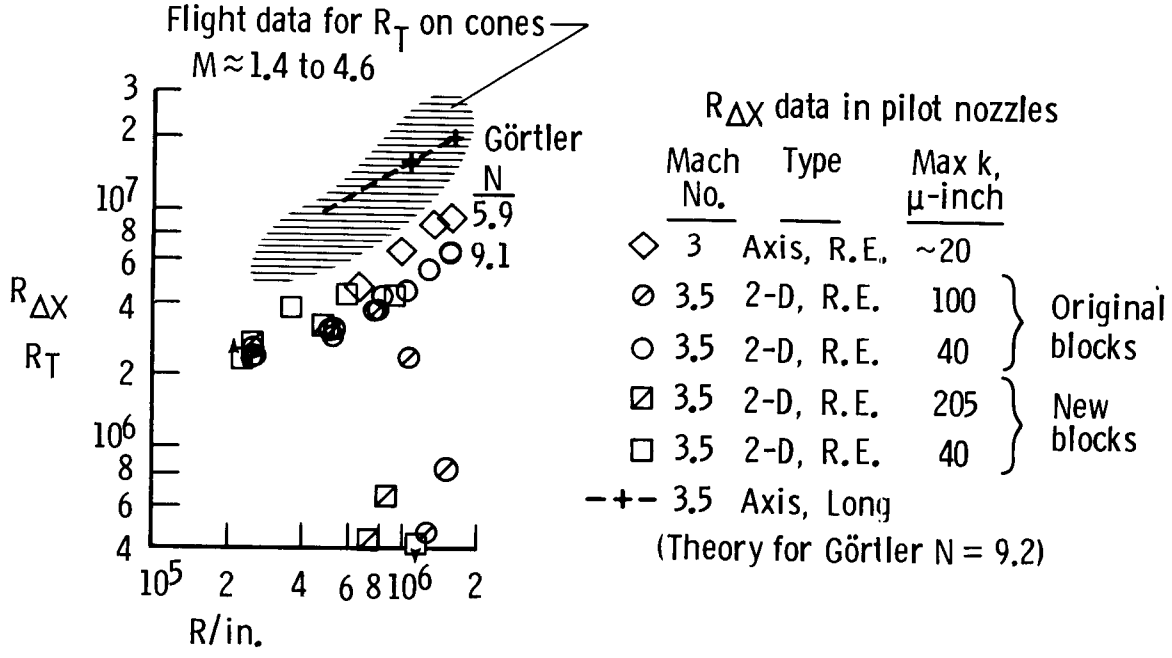

Figure 12

ALLOWABLE SURFACE ROUGHNESS

As a guide for the surface finish specifications on the new Mach 3.5 axisymmetric-long nozzle, values of k have been computed for the same test conditions used for the surface finish assessment of the Mach 3.5 two-dimensional nozzle (fig. 8). Again, values of R_k = 42 and 12 were used as shown in figure 13. For R_k = 12 and at the highest unit Reynolds number this figure indicates that the maximum allowable peak-to-valley roughnesses for this nozzle are increased somewhat to about 50 μ-inches as compared to 40 μ-inches on the two-dimensional nozzle. However, the region where k < 150 μ-inches is required, extends over a total axial distance of about 5.4-inches compared to a corresponding distance of only 1.7-inches on the two-dimensional nozzle.

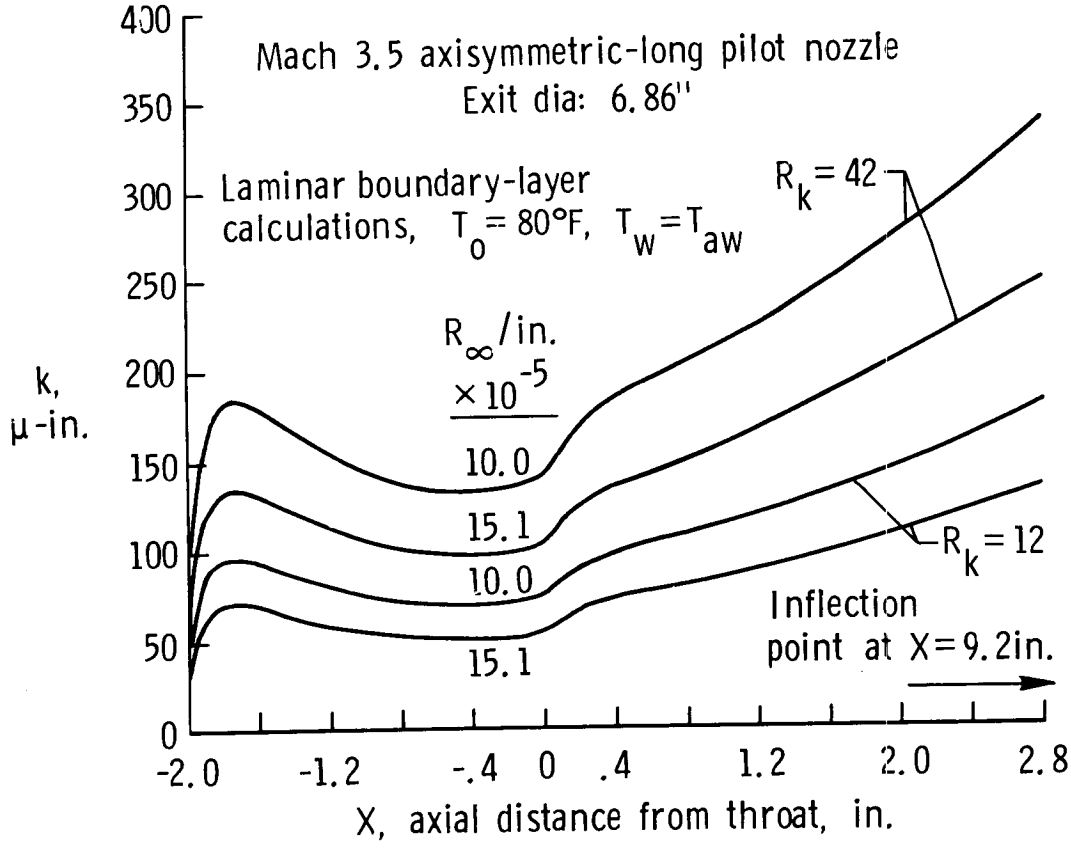

Figure 13

MACH 6 LOW-DISTURBANCE PILOT NOZZLE

A new Mach 6 long-axisymmetric nozzle has been designed using the same radial flow techniques and N-factor criteria as for the new Mach 3.5 axisymmetric nozzle (fig. 11). The engineering design for this nozzle, which will be tested in an existing facility at NASA Langley, is now completed. The contour outline and predicted quiet test core is shown in the upper part of figure 14. The high value of $R_{\infty,\Delta X} = 13.2 \times 10^6$ at $R_\infty/in = 5.1 \times 10^5$ was predicted using N = 9 for transition due to the Görtler instability. At this transition point the value of N for the first mode TS instability was 3.6. In spite of the higher local Mach numbers, the first TS mode was still dominant over the second mode in this calculation. In the lower part of figure 14, the projected performance of the new Mach 6 nozzle, in terms of $R_{\Delta X}$, is compared with Mach 6 transition onset data on cones in atmospheric flight and in conventional wind tunnels. The wind-tunnel data are from references 11 and 12 for 5° and 10° semi-apex angle, sharp tip cones at $M_\infty \simeq 6$. (The data from reference 12 were adjusted to represent transition onset.) The flight data are from figure 4 in reference 13 for cones at $M_e \simeq 6$. The corresponding cross-hatched region in figure 14 is based partly on interpolations along the correlation curves presented in reference 13. Also shown in figure 14 below are experimental values of $R_{\Delta X}$ and corresponding values of N-factors for a Mach 5 axisymmetric, rapid-expansion nozzle tested at NASA Langley (refs. 8 and 10). Again, these comparisons indicate that the new Mach 6 nozzle should provide sufficiently high values of $R_{\Delta X}$ to simulate flight noise levels and transition Reynolds numbers.

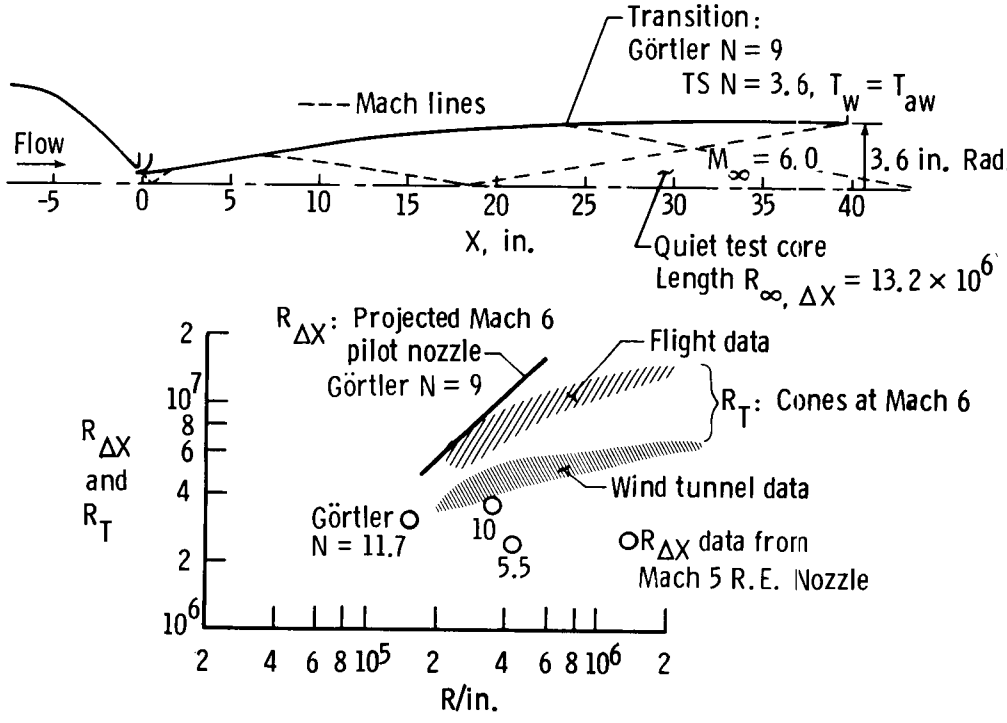

Figure 14

ALLOWABLE SURFACE ROUGHNESS

The values for local roughness Reynolds numbers of R_k = 42 and 12 have again been used to calculate allowable peak-to-valley roughnesses for the new Mach 6 axisymmetric-long pilot nozzle. The results are shown in figure 15 for two unit Reynolds numbers corresponding to stagnation pressures of 150 and 300 psia at the stagnation temperature of 820°R. Thus, for R_k = 12 and $R_\infty/in = 5.1 \times 10^5$, values of k < 30 μ-inches are required in the throat region. This surface finish can be achieved based on our experiences with the Mach 3 axisymmetric nozzle (fig. 12).

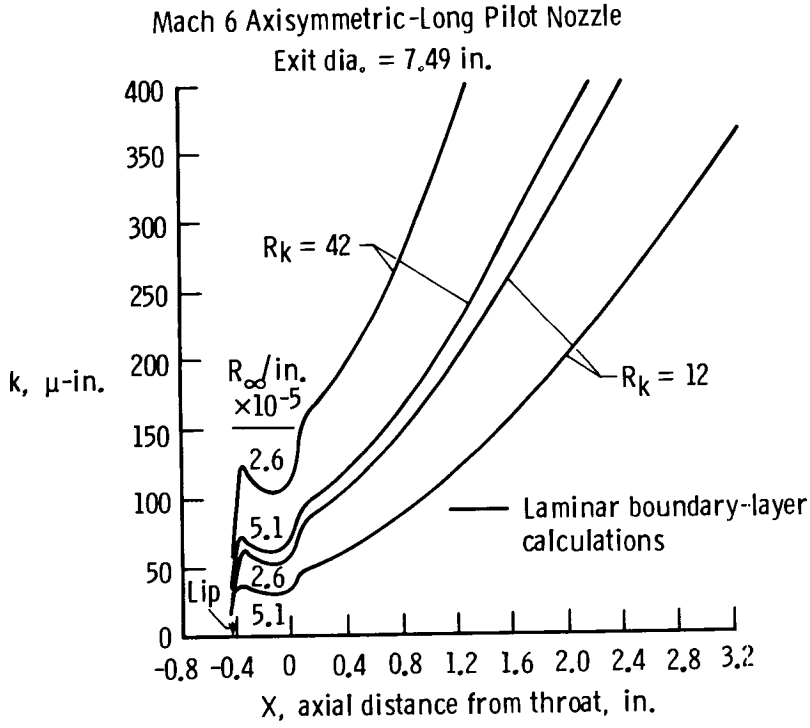

Figure 15

CONCLUSIONS

1. Large width two-dimensional rapid expansion nozzles guarantee wide quiet test cores that are well suited for testing models at large angle of attack and for swept wings. Hence, this type of nozzle will be operated first in the new proposed large scale Supersonic Low-Disturbance Tunnel.

2. Test results indicate that the surface finish of pilot nozzles is critical. The local roughness Reynolds number criteria of $R_k \simeq 10$ will be used to specify allowable roughness on new pilot nozzles and the new proposed tunnel.

3. Experimental data and calculations for M = 3.0, 3.5, and 5.0 nozzles give N-factors from 6 to 10 for transition caused by Görtler vortices.

4. The use of $N \simeq 9.0$ for the Görtler instability predicts quiet test cores in the new M = 3.5 and M = 6.0 axisymmetric-long pilot nozzles that are 3 to 4 times longer than observed in the test nozzles to date. The new nozzles utilize a region of radial flow which moves the inflection point far downstream and delays the onset and amplification of the Görtler vortices.

REFERENCES

1. Creel, Theodore R.; Beckwith, Ivan E.; and Chen, Fang-Jenq: Nozzle Wall Roughness Effects on Free-Stream Noise and Transition in the Pilot Low-Disturbance Tunnel. NASA Technical Memorandum 86389, September 1985.

2. Beckwith, I. E.; Chen, F.-J.; and Creel, T. R., Jr.: Design Requirements for the NASA Langley Supersonic Low-Disturbance Wind Tunnel. AIAA Paper No. 86-0763-CP, March 1986.

3. Beckwith, Ivan E.; Creel, Theodore R., Jr.; Chen, Fang-Jenq; and Kendall, James M.: Free-Stream Noise and Transition Measurements on a Cone in a Mach 3.5 Pilot Low-Disturbance Tunnel. NASA Technical Paper 2180, September 1983.

4. Beckwith, I. E.; Malik, M. R.; and Chen, F.-J.: Nozzle Optimization Study for Quiet Supersonic Wind Tunnels. AIAA-84-1628, June 1984.

5. Chen, Fang-Jenq; Beckwith, Ivan E.; and Creel, Theodore R., Jr.: Correlations of Supersonic Boundary-Layer Transition on Cones Including Effects of Large Axial Variations in Wind-Tunnel Noise. NASA TP-2220, January 1984.

6. Harris, Julius E.; and Blanchard, Doris K.: Computer Program for Solving Laminar, Transitional, or Turbulent Compressible Boundary-Layer Equations for Two-Dimensional and Axisymmetric Flow. NASA Technical Memorandum 83207, February 1982.

7. Braslow, Albert L.: A Review of Factors Affecting Boundary-Layer Transition. NASA TN D-3384, August 1966.

8. Beckwith, Ivan E.; and Holley, Barbara B.: Gortler Vortices and Transition in Wall Boundary Layers of Two Mach 5 Nozzles. NASA Technical Paper 1869, August 1981.

9. Beckwith, Ivan E.; Malik, M. R.; Chen, F.-J.; and Bushnell, D. M.: Effects of Nozzle Design Parameters on the Extent of Quiet Test Flow at Mach 3.5. Laminar-Turbulent Transition, IUTAM Symposium Novosibirsk 1984, Editor: V. V. Kozlov, Springer-Verlag, Berlin, Heidelberg, 1985.

10. Chen, F.-J.; Malik, M. R.; and Beckwith, I. E.: Instabilities and Transition in the Wall Boundary Layers of Low-Disturbance Supersonic Nozzles. AIAA-85-1573, July 1985.

11. Stainback, P. Calvin: Hypersonic Boundary-Layer Transition in the Presence of Wind-Tunnel Noise. AIAA Journal, Vol. 9, No. 12, December 1971, pp. 2475-2476.

12. Pate, S. R.: Measurements and Correlations of Transition Reynolds Numbers on Sharp Slender Cones at High Speeds. AIAA Journal, Vol. 9, No. 6, June 1971, pp. 1082-1090.

13. Beckwith, I. E.: Development of a High Reynolds Number Quiet Tunnel for Transition Research. AIAA Journal, Vol. 13, No. 3, March 1975, pp. 300-306.